Construction of Porous PVDF Coating Layer and Electrochemical Performances of the Corresponding Modified Polyethylene Separators for Lithium Ion Batteries

Li-Feng Fang,[1] Jun-Li Shi,[1,2] Hao Li,[1] Bao-Ku Zhu,[1] Li-Ping Zhu[1]

[1]Department of Polymer Science and Engineering, Key Laboratory of Macromolecule Synthesis and Functionalization, Ministry of Education, Zhejiang University, Hangzhou 310027, People's Republic of China
[2]Ningbo Institute of Material Technology and Engineering, Chinese Academy of Sciences, Ningbo 315201, People's Republic of China
Correspondence to: B.-K. Zhu (E-mail: zhubk@zju.edu.cn)

ABSTRACT: To effectively improve the affinity of polyethylene (PE) separators with liquid electrolyte without causing a serious pore blockage and to develop a more suitable technology for the industrial production process, porous polyvinylidene fluoride (PVDF) layer-coated PE separators are prepared by the dip-coating method followed by a dry-cast process. Different from previous investigations, a less volatile solvent and a relatively volatile nonsolvent are used to yield a preferable pore structure. A brief introduction on the pore formation mechanism during the dry-cast process is provided. The pore structure of coating layer is found to be successfully controlled by changing evaporation temperature, nonsolvent content, and PVDF concentration. The porous PVDF coating layer-modified separators show better affinity with liquid electrolyte and thermal stability. Especially, the ionic conductivity of the modified separator/liquid electrolyte system with a suitable porous coating layer on the separator could reach two times as that of PE separator/liquid electrolyte system, and the cell assembled with modified PE separator shows better cycle performances. This modification process is proved to be a facile, controllable, and effective method for PE separator modification. Meanwhile, this work could provide some theoretical and technical guidance for the production process. © 2014 Wiley Periodicals, Inc. J. Appl. Polym. Sci. **2014**, *131*, 41036.

INTRODUCTION

There is an ever-growing demand for energy sources along with social progress and economy development. Lithium ion battery (LIB), acting as an optional source, is widely used for electronic equipment and electrical vehicles because of its high energy density, long service life, lack of memory effect, and so forth.[1,2] As one of the core components, the separator plays an important role in the ion conduction and avoiding physical contact between the cathode and anode in LIBs. Polyethylene (PE) is one sort of commercialized battery separator materials because of its low price, chemical and thermal stability, and sufficient mechanical strength.[3] However, owing to its intrinsic nonpolar property, the PE separator has poor affinity with polar liquid electrolyte, which could cause relatively low liquid electrolyte uptake, low ionic conductivity, and thus poor cycle performances. Therefore, it is essential to improve the polarity of PE separators to meet the requirements of high performances of LIBs.

Investigators have proposed numerous approaches to enhance polarity of the polyolefin separators, such as surface coating,[4–10] surface grafting,[11,12] and blending.[13–15] On account of the more facile operating process, surface coating is widely adopted. In previous literatures, various materials, such as poly(methyl methacrylate) (PMMA) or its copolymer,[5,6] PMMA/SiO$_2$,[7] poly(vinylidene fluoride-hexafluoropropylene) (PVDF-HFP),[8] and PVDF-HFP/inorganic particles,[9,10] have been coated onto many kinds of common separator. The modified separators show better affinity with liquid electrolyte because of the existence of the polar components. However, the all-covered coating layer usually causes a serious pore blockage and strong resistance for ion transportation. This might then decrease the ionic conductivity of separation-liquid electrolyte system, as well as the cycle performances.[5,16] Therefore, lots of efforts have been done to develop new types of coating layers, which could avoid serious pore blockage. For example, various closely packed nanoparticle-coated separators have been developed.[5,7,9] The
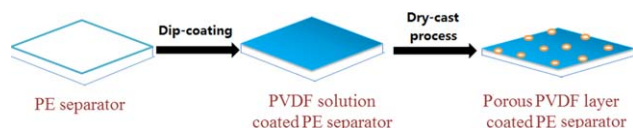
Figure 1. The preparation procedure of the porous PVDF layer-coated PE separator. [Color figure can be viewed in the online issue, which is available at wileyonlinelibrary.com.]

tunnels between the nanoparticles provide a more convenient pathway for the lithium ion transportation. The ionic conductivity of the obtained separator soaked with liquid electrolyte is proved to be higher than that of the all-covered coating layer-modified separator/liquid electrolyte system. Besides, a polydopamine-coated polyolefin separator was also recently reported.[17] Because of the extremely thin modification layer, the pore blockage phenomenon could be ameliorated effectively to some extent. However, although obvious improvement is obtained, this method might not be accepted for the practical application, as the price of dopamine is relatively high.

Fabricating a porous coating layer is another desirable way to solve the aforementioned issues. Therefore, dry-cast process is an effective way to construct porous coating layer. Jeong and Lee[9] and Jeong et al.[18,19] have introduced the porous PVDF-HFP/Al_2O_3 and PVDF-HFP/SiO_2 coating layer onto the separators via this method. Huang and Hitt[2] have prepared a porous PVDF coating layer on an inorganic fiber-based composite separator. In their work, acetone and water were chosen as solvent and nonsolvent, respectively. The porous coating layer of the separators resulted in higher ionic conductivity and better electrochemical performances. In this work, the preferable porous PVDF coating layer was constructed by using a less volatile solvent [industrially commonly used N,N-dimethyl formamide (DMF)[20]] and a relatively volatile nonsolvent (water). We provided a brief introduction on the formation mechanism of the pore structure of the coating layer. The pore structures of coating layer were optimized by controlling the evaporation temperature, nonsolvent content, and PVDF concentration in the casting solution. The effect of porous coating layer on the electrochemical properties was investigated and evaluated.

EXPERIMENTAL

Materials
PE separator (thickness, ~19 μm; porosity, ~45%) was generously supplied by Gaoge Company (China). PVDF (HSV 900, M_w = 1,000,000) was obtained from KYNAR, which was dried in vacuum oven at 40°C for 10 h before use. DMF was bought from Sinopharm Chemical Reagent (China), which was dried by CaH_2 and distilled under reduced pressure before use. Electrolyte solution consisting of $LiPF_6$ (1 mol L^{-1}) and mixture solvent (ethylene carbonate: ethyl methyl carbonate: dimethyl carbonate = 1 : 1 : 1, by weight) was purchased from Guotai Huarong Company (China). The ionic conductivity of electrolyte solution was 10.4 × 10^{-3} S cm^{-1}.

Determination of Phase Diagram of PVDF/DMF/Water System
The phase diagram was determined as proposed in the previous literatures.[21,22] First, a series of polymer solution (the mixture of PVDF and DMF) with same concentration were prepared. Then, nonsolvent was slowly added into the polymer solution

with stirring at a high temperature (100°C). The homogeneous solution was kept at 65°C for a few days to observe the final state of the mixture. The weight of water was recorded when the gelation or liquid–liquid demixing occurred. Then, the composition of the gelation point was achieved.

Fabrication of Porous PVDF Layer-Coated PE Separators
The procedure of fabricating porous PVDF layer-coated PE separators is illustrated in Figure 1. A series of casting solutions containing PVDF, DMF, and water were prepared at 65°C. PVDF powder was dissolved in DMF; then, water was added drop by drop. The solution was kept stirred until it was transparent. A series of homogeneous casting solution were prepared, and the optimized solution compositions are listed in Table I. The well-dispersed polymer solution was applied onto both sides of the PE separator by a dip-coating process.

The PVDF solution-coated separators were dried in the oven under certain temperature (65, 80, and 100°C) to evaporate the solvent and nonsolvent and to induce pores on the coating layer. The prepared separators were then kept in dry desiccator for further use. As shown in Table I, the obtained modified separators treated at 65°C were coded as S5-7, S5-10, and S7-10 corresponding to different casting solutions, respectively.

Characterizations of the Modified Separators
The surface morphologies of the separators were characterized on a scanning electron microscope (Hitachi S4800, Japan) after sputtering gold (Hitachi E1020, Japan). The mechanical strength of the separator was characterized by a tensile tester (RG NF4002, China). The tensile rate was kept at 20 mm min^{-1}, and each sample was cut into the size of 10 mm × 30 mm for the measurement. The thermal stability of the separators was characterized as follows. The separators (15 mm × 15 mm) were placed in the oven at a specific temperature (110, 120, 130, 140, 150, 160, 170, and 180°C) for 1 hour, and the sizes of the separators were recorded. Gurley value was defined as the time for a fixed volume (30 mL) of gas (nitrogen) to pass through separator with certain area (0.79 cm^2) under a pressure (0.02 MPa) on homemade equipment. The liquid electrolyte uptake (ΔW, in percent) was measured by determining the difference in the weights of separators before and after being immersed in the liquid electrolyte for 24 h at room temperature in a glove box filled with argon and was calculated according to the following equation:

$$\Delta W(\%) = \frac{W_w - W_d}{W_d} \times 100 \qquad (1)$$

where W_w and W_d are the weights of the initial saturated weight after absorbing liquid electrolyte and dry separators (in grams),

Table I. The Compositions of the Casting Solutions and the Corresponding Modified Separators

Casting solution number	PVDF (wt %)	DMF (wt %)	Water (wt %)	Separators number
C5-7	5.0	88.3	6.7	S5-7
C5-10	5.0	85.5	9.5	S5-10
C7-10	7.0	83.7	9.3	S7-10

respectively. The retention ratio (R, in percent) of the liquid electrolyte was determined in a dry argon atmosphere at 25°C, which was defined as the ratio of the liquid electrolyte uptake at a specific time and the initial saturated electrolyte uptake. During the whole test process, the activated separators were kept in same sample bags and then taken out to record the weight every few hours. The retention ratio was calculated as follows:

$$R(\%) = \frac{W_t - W_d}{W_w - W_d} \times 100 \qquad (2)$$

where W_t is the weight of the separator when placed aside for a specific time. Ionic conductivity (σ, S cm^{-1}) was tested in the form of stainless steel (SS)/liquid electrolyte–separator/SS. Impedance (R_b, in ohm) was measured on an electrochemical work station system (Princeton Applied Research 2273, PARC) at 25°C over a frequency range of 1 Hz to 10^5 Hz at an amplitude of 5 mV. The σ was calculated by the following equation:

$$\sigma = \frac{d}{R_b \cdot A} \qquad (3)$$

where d and A are the thickness (in micrometers) and effective area (in centimeter squared) of the separator, respectively.[23,24] The interfacial resistance and cycle performances were determined in the form of the cells with LiFePO$_4$ cathode and lithium anode. The interfacial resistance was tested the same as R_b was tested. The cycle performances were obtained on battery test equipment (LAND CT2001A, China) in the voltage range of 2.5–4.2 V at room temperature.

RESULTS AND DISCUSSION

Analysis of the Phase Separation Behavior

Dry-casting process is one kind of common method to prepare porous membranes. In this process, polymer solution with solvent/nonsolvent mixture is casted into film. Generally, the solvent is volatile, whereas the nonsolvent being less volatile. Then, the film is left in air or in a heated oven for a preferential evaporation of the solvent, yielding a phase separation. When the solvent and nonsolvent completely evaporate, the location of nonsolvent in the phase separation process become pores and the porous membrane is obtained.[25] The pore structure is directly affected by the thermodynamic properties of the polymer/solvent/nonsolvent ternary system, and thus, it is important to analyze the phase diagram to achieve a deep understanding on the resultant morphology.

The ternary phase diagram of the mixture of PVDF/DMF/Water was investigated as shown in the Figure 2. The gelation curve (labeled as square) corresponds to the initial composition of the semi-crystalline polymer solution for solid-liquid phase separation during the dry-cast process.[25] On the left side of gelation curve, the mixture is a homogenous fluid; while on the right side, the mixture becomes gel due to the crystallization of PVDF and shows high viscosity. Usually, the addition of nonsolvent (water) induces the polymer to crystallize at low concentration and then the crystallographic PVDF would act as the physical joint point to weaken the motion of the solution. Finally, globular particles would be generated on the coating layer due to solid-liquid phase separation process.[26] However,
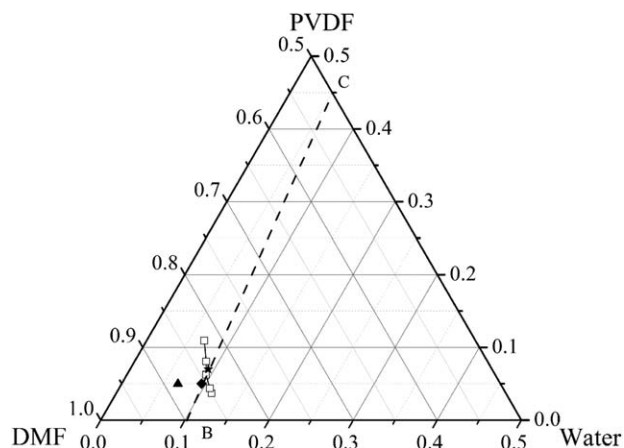

Figure 2. The phase diagram of PVDF/DMF/water system at 65°C (square); BC is computed binodal curve; triangle, C5-7; diamond, C5-10; star, C7-10.

according to previous work,[22] the gelation curve and liquid-liquid de-mixing curve, which is represented by the dash line in Figure 2, coexist at low polymer concentration when the dry-cast temperature is relatively high (65°C or even higher). So the final pore structure of the coating layer might be different.

The boiling points of DMF and water are 149°C and 100°C, respectively. In the dry-cast process, as the treated temperature is relatively low (e.g., 65 and 80°C), the volatile rate for the solvent and nonsolvent might be deemed as being similar or even faster due to the larger area exposed to air. The polymer concentration is gradually increased as a result of evaporation of the solvent and nonsolvent; the solution composition tends to cross the gelation curve; PVDF in the coating layer begins to crystallize (precipitation in casting solution), and the solid–liquid phase separation would occur. A spherulite pore structure is expected for the PVDF coating layer. However, when the initial compositions of the casting solutions in the phase diagram are near to the binodal (especially for casting solution with low polymer concentration), which is critical condition for liquid–liquid demixing (Figure 2), liquid–liquid demixing is preferred to occur during evaporation process. On one hand, high temperature is unfavorable for the crystallization of PVDF, that is, solid–liquid phase separation is depressed. On the other hand, the addition of nonsolvent promotes the liquid–liquid demixing.[22] When a liquid–liquid demixing process occurs prior to solid–liquid phase separation, a spongy-like/cellular pore structure would be formed. Nevertheless, solid–liquid phase separation and liquid–liquid demixing process take place simultaneously, thus, a combination structure tends to be obtained.[27]

Effect of Evaporation Temperature on the Pore Structure

Evaporation temperature is an important factor in the dry-cast process. On one hand, the temperature would have a great impact on pore structure of coating layer, which would further influence the electrochemical performances of the modified separators. For example, Young et al.[26] found that the high evaporation temperature would restrict the growth of nuclei. Thus, the obtained PVDF membrane seemed dense when the particles (nuclei) were driven together to disappear the boundary. On

the other hand, the evaporation temperature directly affects the evaporation rate (determined by evaporation time) of solvent and nonsolvent. Viewed from the industrial production process, the shorter the evaporation time, the higher is the productivity. Therefore, combining both sides of the factor, the determination of the optimized evaporation temperature is of great importance.

To explore the influence of evaporation temperature, PVDF-coated PE separators were dried at different temperatures, and the composition of casting solution was fixed at C5-7. The evaporation temperature was set at 65, 80, and 100°C. As shown in Figure 2, the composition of C5-7 is on the left side of gelation curve, indicating that the initial state of the casting solution is homogeneous at 65°C. For elevated temperature, the gelation curve would move toward the PVDF–Water axis,[22] which means that the initial casting solution/coating layer could still be homogeneous. It is the foundation for fabricating a uniform pore structure on the separator.

The evaporation time and the morphologies of the separators under different evaporation temperatures are shown in Figure 3. The evaporation time is determined as follows. During the dry-cast process, the casting solution-coated PE separators are weighed at regular intervals. The time is recorded until the weight keeps unchanged. As can be seen, the evaporation time is shortened when the evaporation temperature is elevated. Considering the productivity, higher evaporation temperature is preferred. However, it is found that the coating layer is denser [Figure 3(b)] when dried at higher evaporation temperature (80 and 100°C), which is the same as the results reported by Young et al.[26] The reasons lie in that the fast evaporation for the solvent and nonsolvent prevents both liquid–liquid and solid–liquid phase separation. However, when the casting solution is dried at 65°C, both of liquid–liquid and solid–liquid phase separation are sufficiently developed. Therefore, spongy-like pore structure is formed [Figure 3(b)]. As discussed above, the reason for this kind of pore structure is that the initial composition of the casting solution in the phase diagram is close to the binodal curve and that the liquid–liquid demixing process occurred prior to the solid–liquid phase separation. It should be noticed that the pore structure of the coating layer obtained at 65°C is different from previous reports. In the work of Jeong et al.,[10] the coating layer showed a cellular pore structure with many separated open pores, and the porosity is relatively low when acetone and water were used as solvent and nonsolvent, respectively. Comparatively, the pore structure prepared with DMF and water in this work would be more favorable for the improvement of the electrochemical performances of the modified separators because of its connectivity of pore structure and higher porosity, which are crucial factors for liquid electrolyte uptake and ion conduction.

Considering the evaporation time and pore structure, we conclude that 65°C is the optimized operation temperature for the preparation of porous PVDF layer-coated PE separator.

Effect of Nonsolvent Content on the Pore Structure

The nonsolvent content is another key factor influencing the structure of coating layer according to the theory of dry-cast technique.[25] The morphology of the pure PE separator is shown
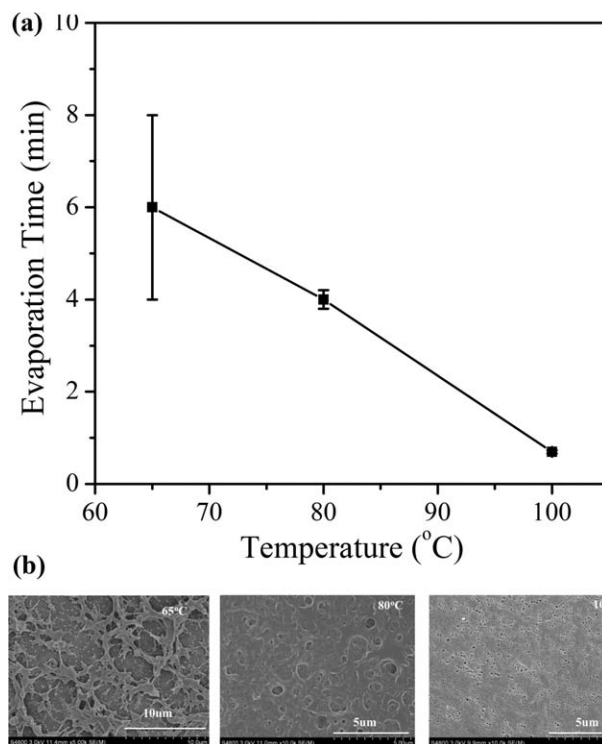

Figure 3. (a) The evaporation time for the modified separators under different evaporation temperatures. (b) The SEM images of the coating layer prepared under different evaporation temperatures (65, 80, and 100°C).

in Figure 4(a). The PVDF concentrations of casting solutions are fixed at 5 wt %, whereas different amount of water (C5-7 and C5-10) is added. As shown in Figure 4(b, S5-7) and Figure 4(c, S5-10), both of the coating layers show a spongy-like pore structure, which is induced by the liquid–liquid demixing, and the surface porosity of the coating layer increases with increasing water content. The difference could be explained as follows. During the dry-cast process, the solvent and nonsolvent evaporate simultaneously at 65°C. The remaining nonsolvent in the solidified PVDF matrix increases with the increasing nonsolvent content in casting solution, resulting in a higher surface porosity in the coating layer. It is the same as reported in the previous literature.[25] Generally, higher surface porosity would result in better connectivity for the modified separators, which is further confirmed by Gurley value in latter discussion.

Effect of PVDF Concentration on the Pore Structure

To investigate the effect of PVDF concentration, the modified separators with the casting solution C5-10 and C7-10 are compared. The final coating layers prepared with C5-10 [Figure 4(c)] and C7-10 [Figure 4(d)] show spongy-like pore structure, suggesting that liquid–liquid demixing process occurs prior to the solid–liquid phase separation process in the dry-cast process. Furthermore, as the porosity of the coating layer is mainly determined by nonsolvent content,[10] lower water content in the casting solution (C7-10) yields a relatively denser coating layer (further proved by Gurley value tests below).

Based on the above analysis, the porous PVDF coating layer could be successfully prepared and effectively controlled by
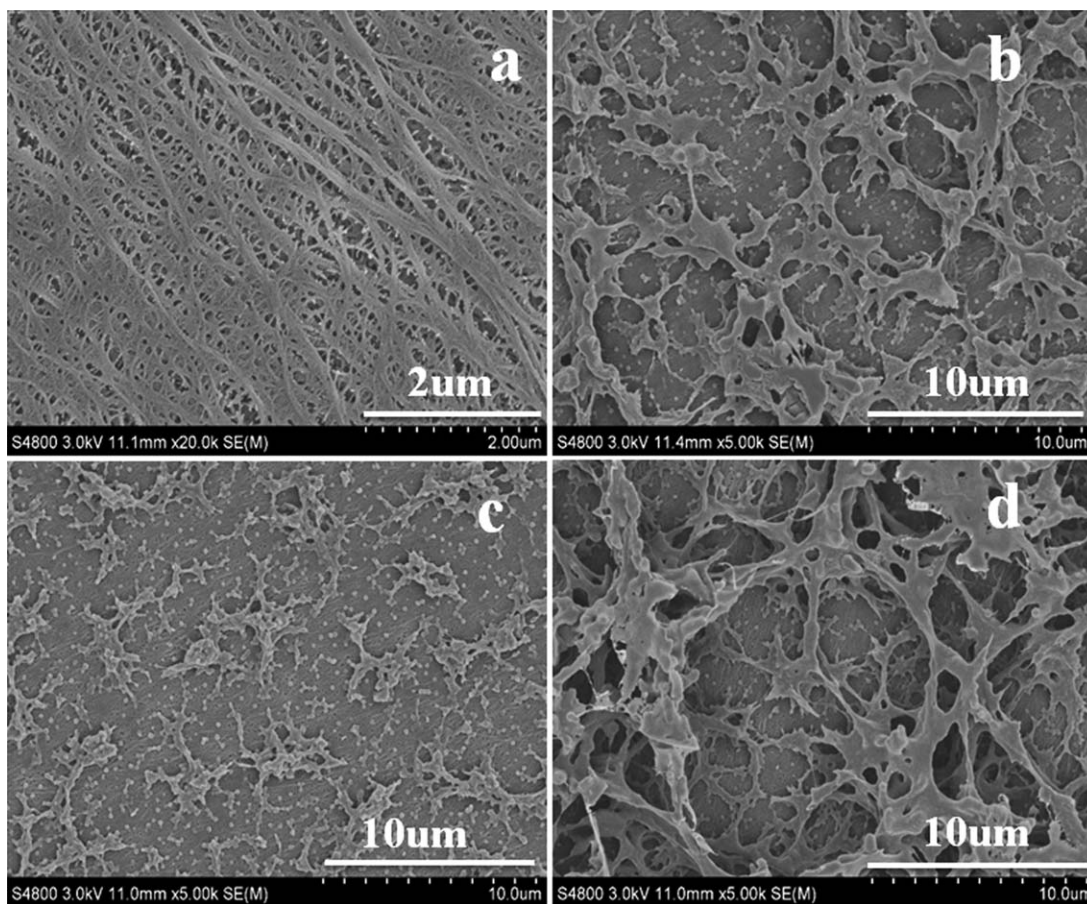
Figure 4. The SEM images of the pure PE separator (a) and the modified separators with different casting solutions: (b) S5-7; (c) S5-10; and (d) S7-10.

changing the evaporation temperature, nonsolvent content, and PVDF concentration in casting solution. These preliminary explorations might provide some theoretical and technical guidance for the production process.

Mechanical Property of the Separators

To evaluate the mechanical property of separators, both of PE separator and S5-10 were characterized by a tensile tester, and the results are listed in Table II. The pure PE separator is fabricated via thermal-induced phase separation process followed with a biaxial stretching process. The longitudinal direction is defined as the same direction with extrusion; and transversal direction is perpendicular to the extrusion direction. Obviously, the tensile strength and elongation ratio of both directions of S5-10 are nearly the same as that of the pure PE separator, which indicates that the modification process is mild and would not damage the mechanical strength of the substrate separator, and the modified separators could satisfy the requirement of LIBs.

Thermal Stability of the Separators

The thermal stability of the separators is the important issue pertaining to not only the battery performance but also safety. If the separators shrink severely during cell cycling especially under high power output conditions, electrodes would contact directly and thus lead to fire or even explosion issues. Thus, the thermal stability of the separators was also carefully studied, and the results are shown in Figure 5. When the temperature exceeds the melting point of PE (132-135°C), the shrinkage of pure PE separator is nearly 100%. However, the shrinkage of PVDF-coated PE separator is still below 60% when the temperature is up to 150°C, which is due to the higher melting point of PVDF ($\sim$ 172°C). The result indicates the enhanced thermal stability of PVDF-modified separators.

Wettability and Liquid Electrolyte Uptake by the Separators

The wettability of the separators is observed by dropping the liquid electrolyte on the surfaces directly, presented in Figure 6. The pure PE separator could not be completely wetted by the liquid electrolyte, and it just acts as an inert skeleton. However,

Table II. Comparison of the Mechanical Properties of PE Separator and the Modified Separator S5-10

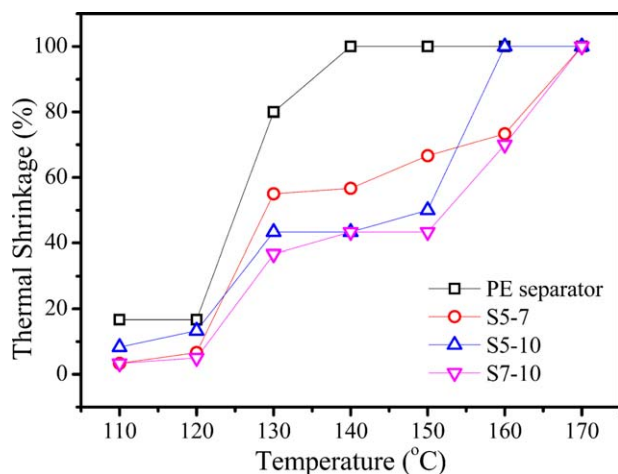| Separator number	Longitudinal		Transversal	
	Tensile strength (MPa)	Elongation ratio (%)	Tensile strength (MPa)	Elongation ratio (%)
PE separator	154	255	92	292
S5-10	148	283	97	293

Figure 5. Thermal shrinkage of PE separator, S5-7, S5-10, and S7-10. [Color figure can be viewed in the online issue, which is available at wileyonlinelibrary.com.]

for S5-10, the liquid electrolyte spreads over the separator after being loaded onto the surface, and the separator turns into transparent immediately. The obviously improved wettability is ascribed to the enhanced affinity between porous PVDF coating layer and liquid electrolyte. The strongly electron-withdrawing functional groups (—C—F—) exist in PVDF, which is similar with polar carbonate esters in liquid electrolyte and it makes easy for PVDF swelling in liquid electrolyte. Moreover, the porous structures enlarge the contact area of coating layer and liquid electrolyte, which further enhances the affinity between separator and liquid electrolyte. Both factors are beneficial for the capillary intrusion of liquid electrolyte into micropores of PE matrix.[18]

The liquid electrolyte uptake by the separator and the stability of liquid electrolyte entrapped in the separator are important factors affecting the electrochemical performances of the separators applied in batteries. The former reflects the interaction between the separator and liquid electrolyte and directly influences the ionic conductivity of the separator–liquid electrolyte system, whereas the latter is relevant to capacity retention ratio
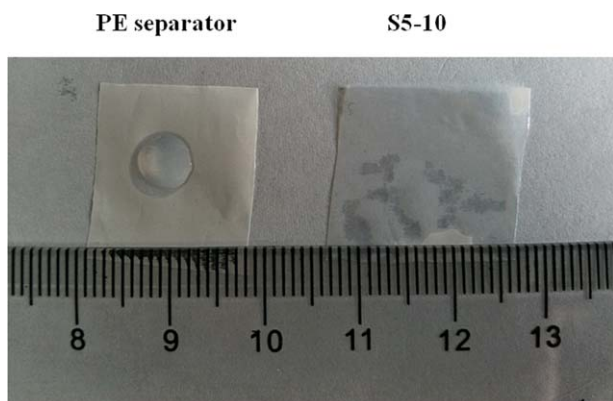
and better battery safety.[11,28] The liquid electrolyte uptakes by the pure PE separator and porous PVDF-coated PE separators and their retention ability are listed in Figure 7. The uptake by PE separator is only 38.0%, whereas that by PVDF-coated separators increases remarkably (e.g., 134.7% for S5-7 and 205.1% for S7-10). The improvement in the uptake is owing to the introduction of the porous PVDF coating layer. The stronger interaction between the separator and liquid electrolyte, which is proved by wettability characterization, results in the higher uptake. For the inert PE separator, the liquid electrolyte occupies the tunnels and pores in the matrix. However, for the PVDF-coated PE separator, liquid electrolyte not only exists in the tunnels and pores of PE matrix and PVDF layer but also can be entrapped by PVDF resin to form gel electrolyte.[29] The higher surface porosity of S5-10 than S5-7 (according to SEM analysis) leads to the higher uptake. The uptake of S7-10 reaches up to 205.1%, which is due to higher PVDF amount and better developed pore structure. The high electrolyte uptake by PVDF coated separators are expected due to the high ionic conductivity.
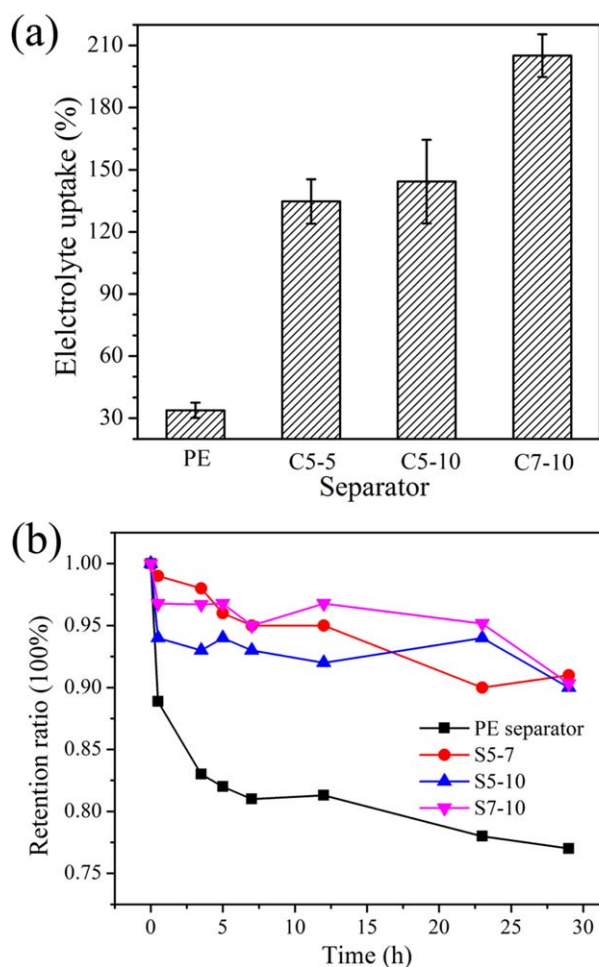

Figure 6. The photograph of the PE separator and S5-10 after dropping the liquid electrolyte on the separator surfaces. [Color figure can be viewed in the online issue, which is available at wileyonlinelibrary.com.]

Figure 7. (a) The liquid electrolyte uptake by PE separator and PVDF-coated PE separators (S5-7, S5-10, and S7-10). (b) The change of electrolyte retention ratio in the separators with time. [Color figure can be viewed in the online issue, which is available at wileyonlinelibrary.com.]
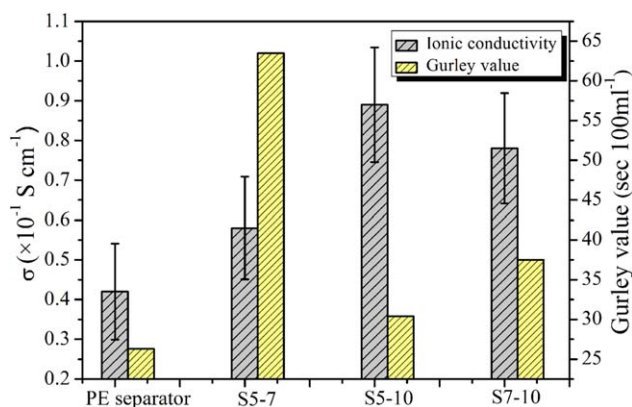
Figure 8. The ionic conductivities and the Gurley values of the pure PE separator and the modified separators (S5-7, S5-10, and S7-10). [Color figure can be viewed in the online issue, which is available at wileyonlinelibrary.com.]

The stability of liquid electrolyte entrapped in separators is displayed in Figure 10. After 30 h, the retention ratio of PE separator decreases to 78%, whereas that of the modified separator stays as high as 90%. The reason for better retention ability is mainly due to the better affinity between porous PVDF coating layer-modified separator and liquid electrolyte. The liquid electrolyte could easily leak out of PE separator because of its low polarity nature. However, the liquid electrolyte entrapped in the porous PVDF coating layer could be divided into two parts, that is, one part is the free liquid electrolyte existing in the pore structure, and the other part is the liquid electrolyte in PVDF gel. The PVDF gel existing on separator surface would prevent the liquid electrolyte from leakage due to enhanced interaction. It would be beneficial for the stability of the entrapped liquid electrolyte. The enhanced retention stability of liquid electrolyte is beneficial for the cycle performances and safety of LIBs.[24,30]

Ionic Conductivity and Gurley Value of the Separators

The ionic conductivities for the liquid electrolyte-soaked separators and Gurley values of the separators are shown in Figure 8. The ionic conductivity of S5-10 reaches up to 0.89×10^{-3} S cm^{-1} at 25°C, which is higher than that of the pure PE separator (0.42×10^{-3} S cm^{-1}). The improvement is because of the higher liquid electrolyte uptake and good pore connectivity of the coating layer. As given in Figure 7(a), the uptake by modified separators is 3–5 times higher as that by pure PE separator, which means higher lithium ion amount in the wetted separators. Besides, pore structure/connectivity is another factor that influences the diffusivity of lithium ions.[31,32] To characterize the pore connectivity of the separators, Gurley value was measured. Gurley value is defined as the time for a fixed volume of nitrogen to pass through separator with certain area under a specific pressure on home-made equipment, which reflects the tortuosity of the pores, when the porosity and thickness of the separators are fixed. The low Gurley value presents the high air permeability,[32,33] implying low diffuse resistance for transmitting lithium ions.[14] As illustrated in Figure 8, all modified separators show higher Gurley value than pure PE separator due to the existence of the coating layer. However, S5-10 possesses the lowest Gurley value among the modified ones due to the

highest porosity of the coating layer as discussed previously. The Gurley value of S5-10 is similar with that of the PE separator, which suggests that the construction of the porous coating layer could effectively avoid serious pore blockage. Therefore, S5-10 shows the highest ionic conductivity. This result is different from that of the report by Jeong et al.[10] The modified separators showed lower ionic conductivity than the unmodified ones in their work because of the relatively thick coating layer and low porosity. In brief, the prepared porous coating layer not only elevates the wettability and the uptake but also avoids pore blockage effectively, yielding higher ionic conductivity.

Electrochemical Performances of the Cells

The electrochemical performances of the cells with S5-10 and S7-10 (with high ionic conductivity) were studied. As shown in Figure 9(a), the initial capacities of the cells with PE, S5-10, and S7-10 are similar to each other. These results are consistent with other literatures.[7,8] The capacity retentions of the cells assembled with PE, S5-10, and S7-10 at room temperature are displayed in Figure 9(b). Obviously, cells containing modified separators exhibit better capacity retention. After 120 cycles, the capacity retention ratios of the cells with PE, S5-10, and S7-10 are 54.0, 71.7, and 74.8%, respectively. It could be interpreted
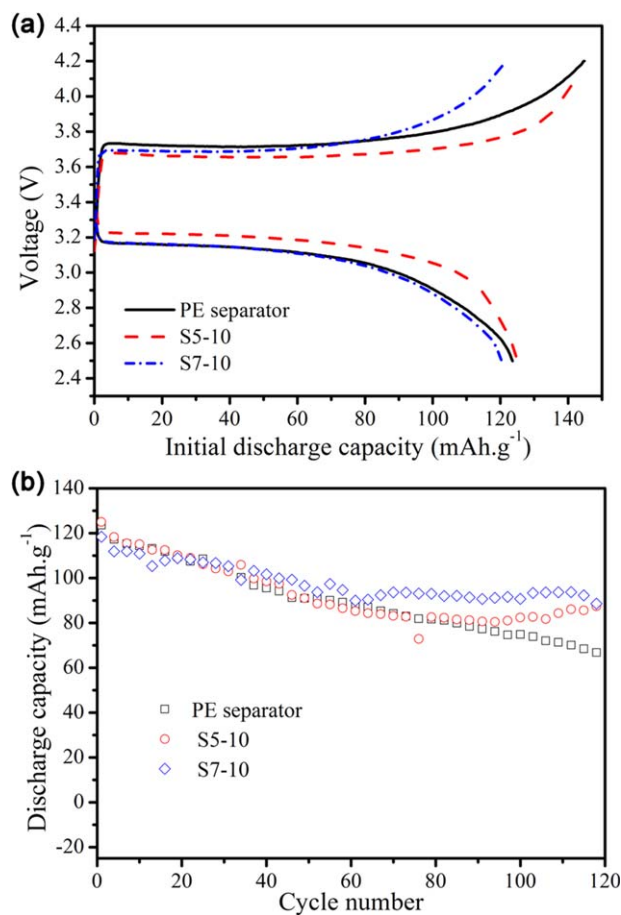

Figure 9. (a) The initial charge/discharge capacities and (b) the discharge capacities as a function of the cycle number of the cells containing PE separator, S5-10, and S7-10. [Color figure can be viewed in the online issue, which is available at wileyonlinelibrary.com.]
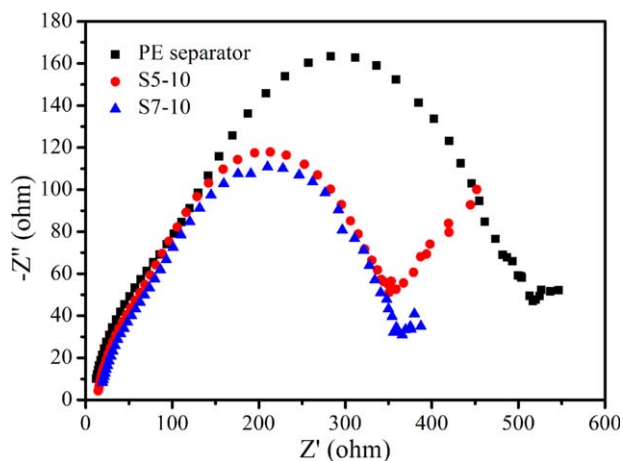
Figure 10. Comparison of the interfacial resistances of cells containing PE separator, S5-10, and S7-10 after 120 cycles. [Color figure can be viewed in the online issue, which is available at wileyonlinelibrary.com.]

as follows. The formation of SEI layer consuming the lithium ions in electrolyte and polarization at electrolyte–electrode interface at high charge/discharge rate attribute to decreased capacities.[28,34–36] However, for S5-10 and S7-10, the higher ionic conductivity results in the lower polarization at electrolyte–electrode interface at relatively high rate (e.g., 1.0 C), yielding the better cycle performance.[34] Otherwise, the increased electrolyte retention ratio of the separators would also improve the capacity retention.[30]

Additionally, the interfacial resistance of the cells after cycling was measured for further investigation on the better capacity retention of the cells assembled with S5-10 and S7-10, and the data are displayed in Figure 10. The semicircle in the Nyquist plot represents the interfacial resistance,[32] and small semicircle means a low interfacial resistance. Obviously, the interfacial resistances of the cells with S5-10 and S7-10 are lower than that of the cell with PE separator due to the intimate contact between the separator surface and the electrodes,[4] suggesting the lower resistance for lithium ions diffusion through the interface layer. Moreover, the cells after cycling were resolved and the separators were compared, as displayed in Supporting Information Figure S1 (S7-10 was taken as an example). It can be seen in Supporting Information Figure S1(a) that the PE separator could be easily taken away from the electrodes, whereas S7-10 is adhered firmly to the cathode/anode and could not be peeled off directly. The photographs of PE separator and S7-10 [Supporting Information Figure S1(b)] after 120 cycles were also compared. Obviously, much more LiFePO$_4$ is adsorbed onto S7-10 than pure PE separator, indicating better affinity between the separator and electrodes. Therefore, the porous PVDF coating layer would enhance the affinity between the separator and electrodes, resulting in a lower interfacial resistance and better cycle performances.

CONCLUSIONS

In this work, porous PVDF coating layer was constructed by dry-cast process. Different from previous researches, less volatile solvent and relatively volatile nonsolvent were adopted, yielding

an ideal pore structure for separator modification. The existence of pores in the coating layer was proved to effectively avoid serious pore blockage for the substrate separator. The porous coating layer could be prepared at relatively low temperature (65°C), and the pore structure could be well controlled by changing the nonsolvent content and PVDF concentration. Considering the simple treatment process, the modification method could be industrialized easily. Meanwhile, the preliminary exploration on the pore structure adjustment might provide some theoretical and technical guidance for the production process. The porous PVDF coating layer-modified PE separators exhibited excellent affinity with liquid electrolyte, enhanced thermal stability, higher liquid electrolyte uptake, higher ionic conductivity, and improved cell performances in comparison with the pure PE separator. These advantageous characteristics indicated a facile and effective method to construct the porous coating layer and to improve the performances of the separators.

REFERENCES

1. Lu, L.; Han, X.; Li, J.; Hua, J.; Ouyang, M. *J. Power Sources* **2013**, *226*, 272.

2. Huang, X.; Hitt, J. *J. Membr. Sci.* **2013**, *425*, 163.

3. Ryou, M.-H.; Lee, Y. M.; Park, J.-K.; Choi, J. W. *Adv. Mater.* **2011**, *23*, 3066.

4. Jeong, Y.-B.; Kim, D.-W. *J. Power Sources* **2004**, *128*, 256.

5. Park, J.-H.; Park, W.; Kim, J. H.; Ryoo, D.; Kim, H. S.; Jeong, Y. U.; Kim, D.-W.; Lee, S.-Y. *J. Power Sources* **2011**, *196*, 7035.

6. Jeong, Y.-B.; Kim, D.-W. *Electrochim. Acta* **2004**, *50*, 323.

7. Park, J.-H.; Cho, J.-H.; Park, W.; Ryoo, D.; Yoon, S.-J.; Kim, J. H.; Jeong, Y. U.; Lee, S.-Y. *J. Power Sources* **2010**, *195*, 8306.

8. Kim, K. J.; Kim, J.-H.; Park, M.-S.; Kwon, H. K.; Kim, H.; Kim, Y.-J. *J. Power Sources* **2012**, *198*, 298.

9. Jeong, H.-S.; Lee, S.-Y. *J. Power Sources* **2011**, *196*, 6716.

10. Jeong, H.-S.; Kim, D.-W.; Jeong, Y. U.; Lee, S.-Y. *J. Power Sources* **2010**, *195*, 6116.

11. Li, S.; Gao, K. *Surf. Coat. Technol.* **2010**, *204*, 2822.

12. Gwon, S.-J.; Choi, J.-H.; Sohn, J.-Y.; Ihm, Y.-E.; Nho, Y.-C. *Nucl. Instrum. Methods Phys. Res. Sect. B* **2009**, *267*, 3309.

13. Zhang, C.; Bai, Y.; Sun, Y.; Gu, J.; Xu, Y. *J. Membr. Sci.* **2010**, *365*, 216.

14. Shi, J.-L.; Fang, L.-F.; Li, H.; Liang, Z.-Y.; Zhu, B.-K.; Zhu, L.-P. *J. Membr. Sci.* **2013**, *429*, 355.

15. Wang, H.; Li, H.; Yu, L.; Jiang, Y.; Wang, K. *J. Appl. Polym. Sci.* **2013**, *130*, 2886.

16. Li, H.; Ma, X.-T.; Shi, J.-L.; Yao, Z.-K.; Zhu, B.-K.; Zhu, L.-P. *Electrochim. Acta* **2011**, *56*, 2641.

17. Lee, Y.; Ryou, M.-H.; Seo, M.; Choi, J. W.; Lee, Y. M. *Electrochim. Acta* **2013**, *113*, 433.

18. Jeong, H.-S.; Choi, E.-S.; Lee, S.-Y.; Kim, J. H. *J. Membr. Sci.* **2012**, *415*, 513.

19. Jeong, H.-S.; Hong, S. C.; Lee, S.-Y. *J. Membr. Sci.* **2010**, *364*, 177.

20. Qin, J.-J.; Wong, F.-S.; Li, Y.; Liu, Y.-T. *J. Membr. Sci.* **2003**, *211*, 139.

21. Cheng, L.-P.; Young, T.-H.; Fang, L.; Gau, J.-J. *Polymer* **1999**, *40*, 2395.

22. Cheng, L.-P. *Macromolecules* **1999**, *32*, 6668.

23. Chen-Yang, Y.; Chen, Y.; Chen, H.; Lin, W.; Tsai, C. *Polymer* **2009**, *50*, 2856.

24. Li, H.; Chen, Y.-M.; Ma, X.-T.; Shi, J.-L.; Zhu, B.-K.; Zhu, L.-P. *J. Membr. Sci.* **2011**, *379*, 397.

25. Nguyen, Q. T.; Alaoui, O. T.; Yang, H.; Mbareck, C. *J. Membr. Sci.* **2010**, *358*, 13.

26. Young, T.-H.; Huang, J.-H.; Chuang, W.-Y. *Eur. Polym. J.* **2002**, *38*, 63.

27. Matsuyama, H.; Teramoto, M.; Uesaka, T. *J. Membr. Sci.* **1997**, *135*, 271.

28. Shi, J.-L.; Fang, L.-F.; Li, H.; Zhang, H.; Zhu, B.-K.; Zhu, L.-P. *J. Membr. Sci.* **2013**, *437*, 160.

29. Hwang, K.; Kwon, B.; Byun, H. *J. Membr. Sci.* **2011**, *378*, 111.

30. Lee, J.-R.; Won, J.-H.; Kim, J. H.; Kim, K. J.; Lee, S.-Y. *J. Power Sources* **2012**, *216*, 42.

31. Arora, P.; Zhang, Z. *Chem. Rev.* **2004**, *104*, 4419.

32. Zhang, S. S. *J. Power Sources* **2007**, *164*, 351.

33. Jeong, H.-S.; Kim, J. H.; Lee, S.-Y. *J. Mater. Chem.* **2010**, *20*, 9180.

34. Jeong, H.-S.; Choi, E.-S.; Lee, S.-Y. *Electrochim. Acta* **2012**, *86*, 317.

35. Zhang, S. S. *J. Power Sources* **2006**, *161*, 1385.

36. Park, J.-H.; Kim, J.-S.; Shim, E.-G.; Park, K.-W.; Hong, Y. T.; Lee, Y.-S.; Lee, S.-Y. *Electrochem. Commun.* **2010**, *12*, 1099.